Mechanisms and Machine Science 72

Richard (Chunhui) Yang
Yukio Takeda
Chunwei Zhang
Gu Fang *Editors*

# Robotics and Mechatronics

## Proceedings of the Fifth IFToMM International Symposium on Robotics & Mechatronics (ISRM 2017)

Springer

# Mechanisms and Machine Science

Volume 72

This book series establishes a well-defined forum for monographs, edited Books, and proceedings on mechanical engineering with particular emphasis on MMS (Mechanism and Machine Science). The final goal is the publication of research that shows the development of mechanical engineering and particularly MMS in all technical aspects, even in very recent assessments. Published works share an approach by which technical details and formulation are discussed, and discuss modern formalisms with the aim to circulate research and technical achievements for use in professional, research, academic, and teaching activities.

This technical approach is an essential characteristic of the series. By discussing technical details and formulations in terms of modern formalisms, the possibility is created not only to show technical developments but also to explain achievements for technical teaching and research activity today and for the future.

The book series is intended to collect technical views on developments of the broad field of MMS in a unique frame that can be seen in its totality as an Encyclopaedia of MMS but with the additional purpose of archiving and teaching MMS achievements. Therefore, the book series will be of use not only for researchers and teachers in Mechanical Engineering but also for professionals and students for their formation and future work.

The series is promoted under the auspices of International Federation for the Promotion of Mechanism and Machine Science (IFToMM).

Prospective authors and editors can contact Mr. Pierpaolo Riva (publishing editor, Springer) at: pierpaolo.riva@springer.com.

Indexed by SCOPUS and Google Scholar.

More information about this series at http://www.springer.com/series/8779

Richard (Chunhui) Yang ·
Yukio Takeda · Chunwei Zhang ·
Gu Fang
Editors

# Robotics and Mechatronics

## Proceedings of the Fifth IFToMM International Symposium on Robotics & Mechatronics (ISRM 2017)

Springer

*Editors*
Richard (Chunhui) Yang
Western Sydney University
Penrith, NSW, Australia

Chunwei Zhang
Qingdao University of Technology
Qingdao, China

Yukio Takeda
Department of Mechanical Engineering
Tokyo Institute of Technology
Tokyo, Japan

Gu Fang
Western Sydney University
Penrith, NSW, Australia

ISSN 2211-0984 ISSN 2211-0992 (electronic)
Mechanisms and Machine Science
ISBN 978-3-030-17676-1 ISBN 978-3-030-17677-8 (eBook)
https://doi.org/10.1007/978-3-030-17677-8



This Springer imprint is published by the registered company Springer Nature Switzerland AG
The registered company address is: Gewerbestrasse 11, 6330 Cham, Switzerland

# Contents

# Chapter 1
# Architecture Choice of a Robotic Hand for Deep-Sea Exploration Based on the Expert Gestures Movements Analysis

**C. Mizera, M. A. Laribi, D. Degez, J. P. Gazeau, P. Vulliez and S. Zeghloul**

**Abstract** In this paper, a method to choose the hand architecture of an end effector used for deep-sea exploration will be presented. This method is based on the study of the movements of an archeologist and on the analysis of its recorded gestures. These observations allow an objective description of the archaeologist tasks, which are for the most part specific to this activity. From this preliminary study and from several criteria based on the fingertips workspace and on the quality of grasps, the hand architecture has been defined. To sum up the study of the archeologist gesture, a new taxonomy specific to this activity was established.

**Keywords** Design · Robotic hand · Motion capture · Submarine · Archaeology

## 1.1 Introduction

Human hand specificity is the ability to perform a wide range of grasps with objects of different dimensions, masses, shapes and fragilities. Adaptability and human hand dexterity are the main reasons why robotic grippers try to imitate our hands. Human

C. Mizera · M. A. Laribi (✉) · D. Degez · J. P. Gazeau · P. Vulliez · S. Zeghloul
GMSC Department, PPRIME Institute, University of Poitiers, RoBioSS, CNRS, UPR 3346, Poitiers, France
e-mail: med.amine.laribi@univ-poitiers.fr

C. Mizera
e-mail: camille.mizera@univ-poitiers.fr

D. Degez
e-mail: denis.degez@culture.gouv.fr

J. P. Gazeau
e-mail: jean.pierre.gazeau@univ-poitiers.fr

P. Vulliez
e-mail: philippe.vulliez@univ-poitiers.fr

S. Zeghloul
e-mail: said.zeghloul@univ-poitiers.fr



R. Yang et al. (eds.), *Robotics and Mechatronics*, Mechanisms and Machine Science 72, https://doi.org/10.1007/978-3-030-17677-8_1

grasp has been studied before to have a better understanding of the interaction between objects and hand [1, 2]. This would allow the design of more effective robotic hand that would reproduce human grasp with more precision. The study [3] showed that some grasps are predominant for some activities while not used at all for others. Consequently, an end effector adapted for a specific task or set of tasks will not suit another.

In this paper, we will investigate the geometric design of a robotic hand that would be used for submarine archaeology. For that purpose, we will observe and analyses the gestures of an archaeological expert. Indeed, submarine exploration require specific gestures to extract carefully fragile objects.

Few grippers of different shapes and dexterity level have been designed before for this specific activity. Previous subsea end effectors were quite perfunctory, with only two degrees of freedom like a simple grip, like for example the ORION manipulators or the AMADEUS hand [4], and consequently unsuitable for the manipulation of objects of different shape and fragility. More recent end effectors were made for that purpose, like the HEU Hand [5], the Ocean One hand [6] or the Bologna University hand [7]. These hands are more adaptable to different shapes of objects. Yet, they only have three fingers, with only 2 DOF each for the Bologna University and the Ocean One hand; and with 3 DOF each for the HEU hand. Consequently, they cannot reproduce accurately the delicate and various gestures of the archaeologist. Moreover, due to their restricted dimension, Ocean One and HEU hands can only grasps small objects. Bologna University hand is able to grasp both small and large objects, but it is quite bulky. Only the Bologna University hand have sensors giving an information on the contact forces, which is necessary not to damage fragile objects. Last, these hands are not made to go beyond a 100 m depth.

The paper is organized as follows: Sect. 1.2 presents the analysis of the task made from the recording and the study of the archaeologist gesture. Section 1.3 presents the choice of the hand architecture of the hand, based on the conclusions of Sect. 1.2. Criteria will be defined to evaluate the hand workspace and the quality of the grasp of spherical and prismatic objects. Conclusions and perspectives are presented at the end of the paper.

## 1.2 Analysis of the Archaeologist Gesture

### *1.2.1 Recording of the Motions*

In order to have a better understanding of the submarine archaeology, and to design a robotic hand that would suit this activity, we proceeded to the analysis of the expert's gestures. To do this, we simulated an archaeological site by hiding selected objects in the sand (Fig. 1.1). The objects match the different categories of artefacts we may find on a wreck, and all of them require specific gesture and precaution. Based on the expertise of the archaeologist diver, we selected very small and light objects like

**Fig. 1.1** Experimental site

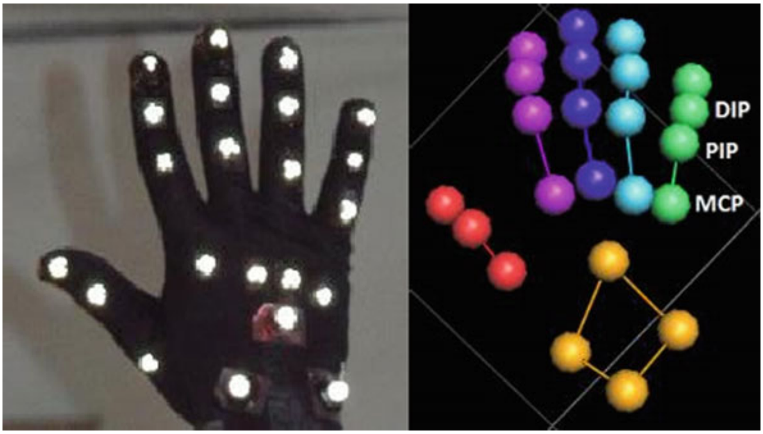


**Fig. 1.2** Position of the markers on the hand

ceramic fragments or bullets, containers, broken ceramic object, bulky and heavy object. We also disposed very fragile objects like what may be found undersea, damaged by time and water.

Motion capture system was used to record the expert gesture. We used ten cameras, MXT40, that record the marker coordinates at a frequency of 100 Hz. Passive markers are placed on the hand and the arm of the archeologist, as depicted on Fig. 1.2. A model composed by 23 markers is considered.

The placement of the markers allows the recording of every motions of flexion/extension and abduction/adduction of the fingers.

Each finger can produce a movement of flexion at the level of the distal interphalangeal (DIP) joint, the proximal interphalangeal (PIP) joint and the metacarpophalangeal (MCP) joint. These joints are represented on Fig. 1.2.

## *1.2.2 Obtained Results*

The conducted motion capture study and the observation of the expert gestures lead to identify two main purposes of the hand in the submarine archaeology context. Firstly, the hand can be used as a gripper, to grasp tools or underwater objects. Secondly, the hand can be used directly as a tool, to search through the sand or to clear objects.

The workspace of the hand was identified, by computing all the points swept by the extremity of the fingers for each task. The flexion angle as well as the joint speed was computed for each joint on the hand.

### 1.2.2.1 Hand Used as a Tool

In these examples, the hand itself is used to perform the action. These observed gestures are quite specifics to submarine archeology.

*Observed gestures*

Sweeping: As a layer of sediments often hides the objects, it is necessary for the archeologist to clear the area in order to bring out objects and facilitate access. The sweeping consists in slowly passing the hand over an object to remove the sand covering it. This action is made without contact, thanks to the water movement. It's important to notice that the expert does not use its thumb during this gesture.
Scratching: When the sweeping is not enough to bring out entirely the desired object, the expert have to scratch delicately the sand around it for the artifact to be completely clear. The action of scratching is made with 1, 2, 3 or 4 fingers depending on the amount of sediment that need to be removed, and on the estimated fragility of the object. The thumb is not used for this gesture.
Shoveling: For shoveling action, the hand is put in flat configuration and slides under the object to lift it without damaging. For that purpose, fingers have to push the sand stuck under the objects.

*Observations*

For each of these actions we notified that:

- The thumb is barely used. It follows passively the other fingers most of the time.
- The flexion movements of the four fingers (index finger, middle finger, ring finger and pinky finger) are almost identical. Nonetheless, the expert do not use its pinky finger every time.

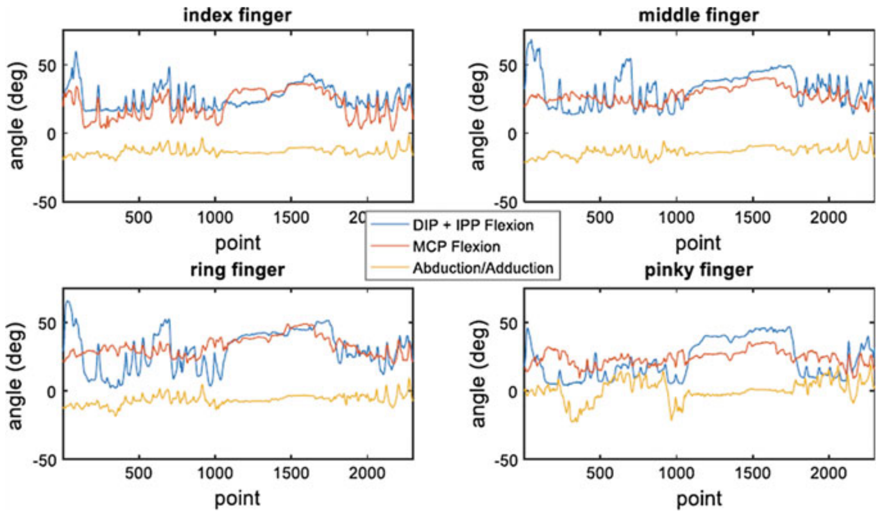


**Fig. 1.3** Evolution of the joint configuration of the hand during the scratching gesture

**Fig. 1.4** Range of abduction of the fingers

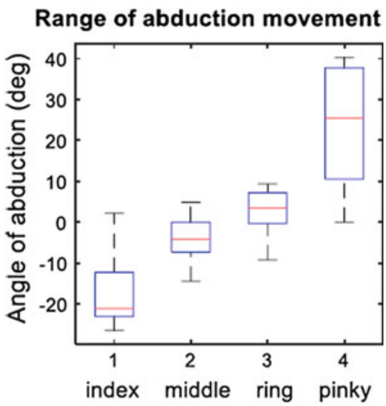


- The MCP flexion as well as the PIP flexion are coupled. The coupling is approximately the same for the four fingers; but the coupling value is different and depend on each action.

Scratching movement as well as sweeping movement do not request abduction/adduction movements of the four fingers (index, middle, ring and pinky). Example of angles evolution during scratching movement are depicted on Figs. 1.3 and 1.4.

By looking at the joint velocity variations, we noticed that the movements are slow. For the scratching and the swiping, the movements of flexion are composed of regular cycles: mean cycle of 750 ms for the scratching gesture and mean cycle

**Table 1.1** Maximal rotational speed recorded

| Joint | Maximum rotational speed recorded (°/s) |
|---|---|
| MCP | 204 |
| PIP | 192 |

of 320 ms for the sweeping gesture. The maximum rotational speed recorded are presented in Table 1.1.

#### 1.2.2.2 Hand Used to Grasp Objects

The hand grasps two categories of objects: the archaeologic artefacts and a wide variety of tools. The gesture realized to grasp tools are well documented in the literature, like in Feix taxonomy [2]. Among them, we can find large tools used in power grasp like hammers or trowel; delicate tools like scalpels or brush in precision grasp; clamp used to seize tiny parts.

These tools are grasped by the handle, which can have various sizes and shapes. We will have the possibility to adapt the shape of the handle of the tools to facilitate the grasping.

Archaeological artefact needs precautions to be lifted. In the next, an atlas of different artefact categories is presented.

*Categories of objects*

Very small objects: The small objects and the fragments are grasped with fingertips, between two or three fingers. It is a precision grasp.
Fragile objects: The very fragile objects, which can disintegrate in the slightest contact, are not directly grasped in the hand. It is necessary to slide a box under the object to bring it to the surface still surrounded with sediments. This operation can be made with one or two hands, knowing that the contents of the box can be heavy because we keep the sand surrounding the object. During the grasp, fingers are placed stretched out under the box and the thumb in opposition locks the grip.
Dislocated objects: The objects likely to come apart, like brush of brooms, are seized compressed between two hands. It is important to cover the largest area possible with the hand, and the fingers are widely spaced in order to secure the grip to the maximum and avoid losing pieces.
Bulky objects: The very heavy or voluminous objects are taken with two hands. Their geometry is very variable. According to their shape and to their fragility, they can either be grabbed from below, with flat hands acting as support, or by sides with hands in opposition. Some of these grips will be achievable with only one larger hand.
Others: The other artefacts, which are the majority, are grabbed inside the palm. For that, there are two possibilities. The hand slides under the object (see the shoveling action) and the fingers deploy around the surface and conform to its shape. The thumb may then be deployed in opposition to secure the grasp. The other scenario is that

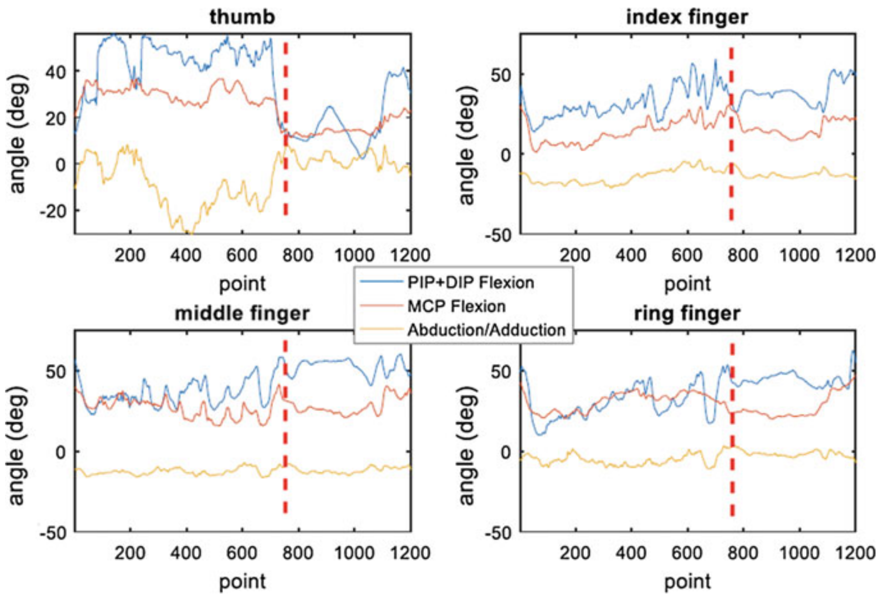


**Fig. 1.5** Evolution of the joint configuration during the grasp of an object

the object is seized by the fingertips and then placed inside the palm thanks to a wrist rotation. The objects can be roughly divided in three categories, according to their shapes: spheres, prism and cylinders.

*Observations*

For each of these gestures we notified that:

- The movement of the wrist is very important to place the hand in relation with the object, and to dispose the object in the palm.
- The flexion of the four fingers (index, middle, ring and pinky finger) are synchronized.
- The MCP flexion and the IPP flexion are coupled, but the coupling value depends on the action.

For example on Fig. 1.5, we can observe the angular variation of the different joints before the actual grasp of the object, on the left of the red line, and when the grasp is effective on the right. We can also observe on this figure that the thumb joint makes important movements to secure the grasp. In most of the grasping motion observed, the thumb is very mobile.

There is few motion of abduction/adduction for the other four fingers during the grasp of the same object type. Nonetheless when switching from an object type to another, the angle of abduction varies significantly.

We observed that the coupling ratio between the PIP flexion and the DIP flexion varies according to the objects being grasped. This ratio does not vary much during

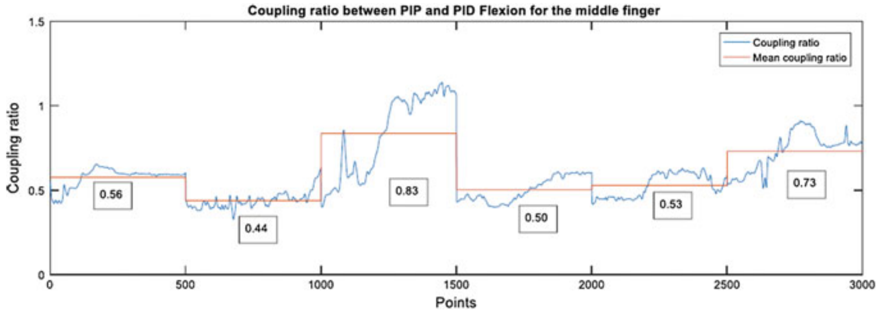


**Fig. 1.6** Coupling ratio between the PIP and the DIP flexion

a same gesture. On Fig. 1.6, we can notice the coupling ratio during the grasp of different objects: a marble, a small ball, a plate, a prismatic box, a bottle and a large bowl.

### *1.2.3 Data Analysis*

The total fingertips workspace observed, for several gestures is represented on Fig. 1.7 relative to the coordinate system represented next to it. The points correspond to the different positions of the fingertips during several gestures: sweeping, scratching, grasping a small object with the fingertips and grasping a larger object in the palm. All these points form the set *WA* that represent the archeologist workspace. It could be contained in half a sphere of 100 mm radius represented on Fig. 1.7 in black. The workspace center is situated 100 mm under the palm, centered relatively to the y-axis with an offset toward the fingertips relatively to the x-axis.

The Table 1.2 gives the total angular range for all recorded motion. The angles of abduction-adduction are measured between the grey line and the line perpendicular to the red line as shown on the figure on Table 1.2.

The analysis of gesture leads to the following conclusions that will be important for the hand design:

- The hand needs to have at least four fingers: three fingers on a side of the hand, and one opposable thumb. Indeed, to lift an object in a flat hand, it is necessary to maximize the contact surface between the hand and the object.
- Different actions are observed through the motion captures, from grasping fragile objects to scratching the sand: the three fingers (index, middle and ring fingers) act always simultaneously.
- It is necessary to have an opposable thumb to perform an efficient grasp. Through the observation of the workspace of the thumb's extremity during the different grasping phases, its movement is preponderant. The observation of the hand's workspace during several movements shows that the thumb should have a wide

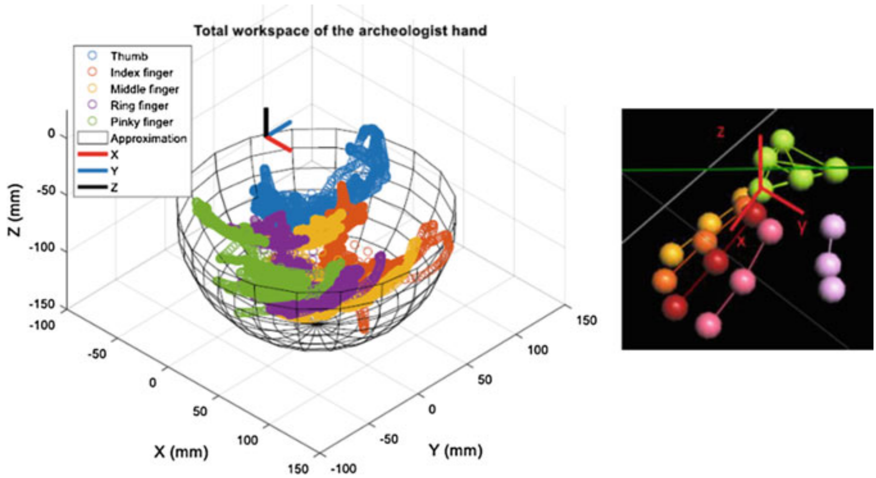


**Fig. 1.7** Total workspace of the archaeologist fingertips

**Table 1.2** Total angular range

| | Thumb (°) | Index finger (°) | Middle finger (°) | Ring finger (°) | Pinky finger (°) | |
|---|---|---|---|---|---|---|
| MCP flexion | 31–68 | 1–38 | 7–47 | 12–62 | 3–60 | 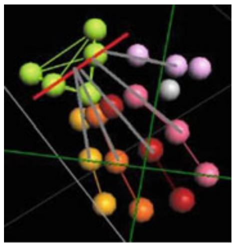 Reference lines |
| PIP + DIP flexion | 2–58 | 8–62 | 9–91 | 2–66 | 0–83 | |
| Abduction/Adduction | −31 to 3 | −32 to 3 | 40–81 | −30 to 7 | −28 to 4 | |

workspace. It should also be able to be in direct opposition with each of the three other fingers. This result was also discussed by Kapandji and led to the Kapandji test [8]. Consequently, the thumb will be able to proceed to a movement of abduction/adduction in addition to the MCP flexion.

- A small amplitude movement of abduction/adduction for the index, middle, ring and pinky fingers during a given gesture of the hand used as a tool or for grasping.
- The angle of abduction-adduction varies widely from a grasping configuration to another. For example, the abduction-adduction angle is much wider for large objects grasps than for small fragments.
- As the contact surface between the fingers and the object is maximized for the grasps (except for the fingertips grasp of the smallest objects), it is better to have at least three phalanges for the finger to conform to the objects shapes.

Based on this analysis, we built a taxonomy of the submarine archaeology activity is presented in annex. All gestures presented above are illustrated in this taxonomy.

## 1.3 Choice of the Hand Architecture

The hand architecture definition consists in this preliminary study in defining the configuration of fingers and thumb on the palm. This definition is based on the evaluation of the workspace of the archeologist hand and on the stability of the object.

Regarding the previous observations, several hand geometries seem to suit the archeologist work with different placements of the thumb, as shown in the Table 1.3. The only joints represented are the one leading to the abduction/adduction motion, and the MCP flexion of the thumb.

Due to the compactness problem and the difficult environmental conditions underwater, the under-actuation is one of the most important constraint to comply.

In order to select the best geometry able to perform the archeologist work an evaluation procedure based on two criterions is proposed. The first criterion concerns the total workspace of the hand, and the second one concerns the ability of the hand to ensure stable grasps.

**Table 1.3** Schemes of the possible hand architectures

| Anthropomorphic (1) | Opposite thumb (2) | Thumb on the palm (3) |
|---|---|---|
| 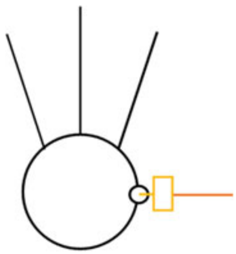 | 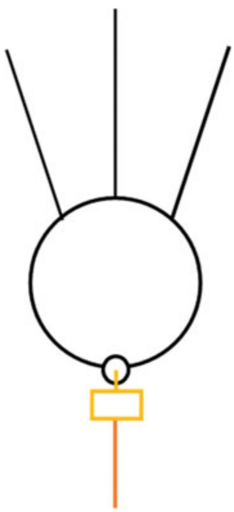 | 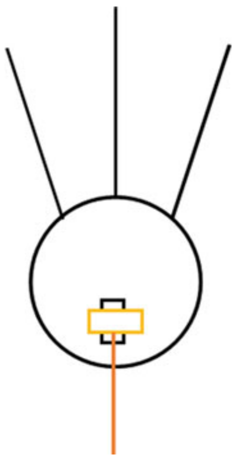 |

### 1.3.1 Total Workspace of the Hand

In this section, the fingertips workspace for each of the 3 investigated hand geometry has been drawn and evaluated. All hand are considered with the same fingers length, palm dimension and joints limits.

The dimensions as well as the joint limits of the considered robotic hand, whose workspace and grasp quality are computed, are summarized up in Table 1.4. The choice of these dimensions was based on a precedent work of the team [9], with a 1.5 factor.

To evaluate the workspaces, we compare them to the discretized workspace of the archeologist hand obtained by motion capture, noted *WA* and represented on Fig. 1.7. It is composed of approximatively 20000 points.

*WA* is the set of points *Pa* reached by the archeologist.

$$Pa(i) \in WA, \quad i = 1, \ldots, n, \quad n \sim 20000 \tag{1.1}$$

*WH* is the set of points *Ph* reachable by the robotic hand. We create this set by calculating the coordinates of the fingertips of the robotic hand. These coordinate are obtained by sweeping, every 5 degrees, all the possible combinations of angular position of the fingers, within the joints limits presented in Table 1.3. We get a set composed of approximatively 25000 points.

$$Ph(i) \in WH, \quad i = 1, \ldots, m, \quad m \sim 25000 \tag{1.2}$$

With,

$$Ph(i) = f\left(q_{1i}, q_{2i}, q_{3i}, \theta_i, q_{1pi}, q_{2pi}, q_{3pi}, \theta_{pi}\right) \quad \text{for} \quad i = 1, \ldots, m, \quad m \sim 25000 \tag{1.3}$$

and, $q_{1i}, q_{2i}, q_{3i}, \theta_i, q_{1pi}, q_{2pi}, q_{3pi}, \theta_{pi}$ the angular parameters of the hand depicted on Fig. 1.10.

One notes that the fingers 1, 2 and 3 are coupled and have consequently the same MCP flexion angle $q_1$, PIP flexion angle $q_2$ and DIP flexion angle $q_3$.

The parameter *r* is defined as a covering ratio and computed as follows.

$$r = \frac{\sum_1^n C_i}{n} \quad \text{With } C_i = \begin{cases} 1 \; if \; Pa(i) \in WH \\ 0 \; if \; Pa(i) \notin WH \end{cases} \tag{1.4}$$

**Table 1.4** Dimensions and joint limits

| $a$ (mm) | $L_1 = L_{1p}$ (mm) | $L_2 = L_{2p}$ (mm) | $L_3 = L_{3p}$ (mm) | $L_{abd}$ (mm) | $\theta c(^\circ)$ | $q_1(^\circ)$ | $q_2(^\circ)$ | $q_{1p}(^\circ)$ | $q_{2p}(^\circ)$ | $\theta(^\circ)$ | $\theta_p(^\circ)$ |
|---|---|---|---|---|---|---|---|---|---|---|---|
| 35 | 75 | 52.5 | 30 | 20 | 45 | [0, 90] | [0, 90] | [0, 90] | [0, 90] | [0, 90] | [−40, 40] |

**Table 1.5** Workspaces of the fingers

| | Anthropomorphic (1) | Opposite thumb (2) | On the palm (3) |
|---|---|---|---|
| Workspace volume | $3.47 \times 10^{-3}$ m$^3$ | $4.03 \times 10^{-3}$ m$^3$ | $6.78 \times 10^{-3}$ m$^3$ |
| Ratio $r$ | 0.931 | 0.946 | 0.982 |
| Workspaces | 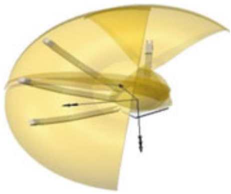 | 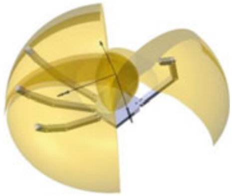 | 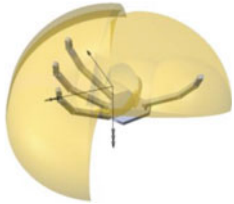 |

The two sets of points *WH* and *WA* are compared. If $r = 1$, it means that all the points reachable by the archeologist hand are reachable by the robotic hand.

The workspaces of the hands and the obtained ratios $r$ are shown on Table 1.5.

It is stressed that the anthropomorphic placement of the thumb is not ideal in term of workspace criterion. This could be explained by superposition of the thumb workspace and the third finger workspace, which reduce the total workspace and leads to possible collision.

The third hand geometry presents a larger workspace, and covers the largest area over the palm. Moreover, this geometry has the largest covering ratio $r$, which means that the placement of the thumb allows to sweep a maximum of the points accessible by the hand of the archaeologist. This ratio will be improved in the future work by optimizing the geometric parameters of the robotic hand.

### *1.3.2 Ability to Make a Stable Grasp*

The quality of a grasp depends mainly on its stability. It can be evaluated with several criterions. In a previous work of the team, these criterions were listed and compared [10].

The three different solutions for the thumb placement are consequently compared over the quality of the fingertips grasps. For that, we qualify the grasp of objects with simple geometric shapes that approximate the archaeologic artefacts. The grasps of spheres with different diameters will be evaluated as well as prisms with different thicknesses. Indeed, human grasps can be divided in two categories: prismatic and circular grasp [1] and this shapes allows the evaluation of these grasps.

Figure 1.8 presents the implemented algorithm to compute the criterion evaluating the grasp quality an object. Several constraints should be validated before computing the grasp quality. These constraints concern the contact between fingertips and object surface, the contact orientation and the force closure constraint.

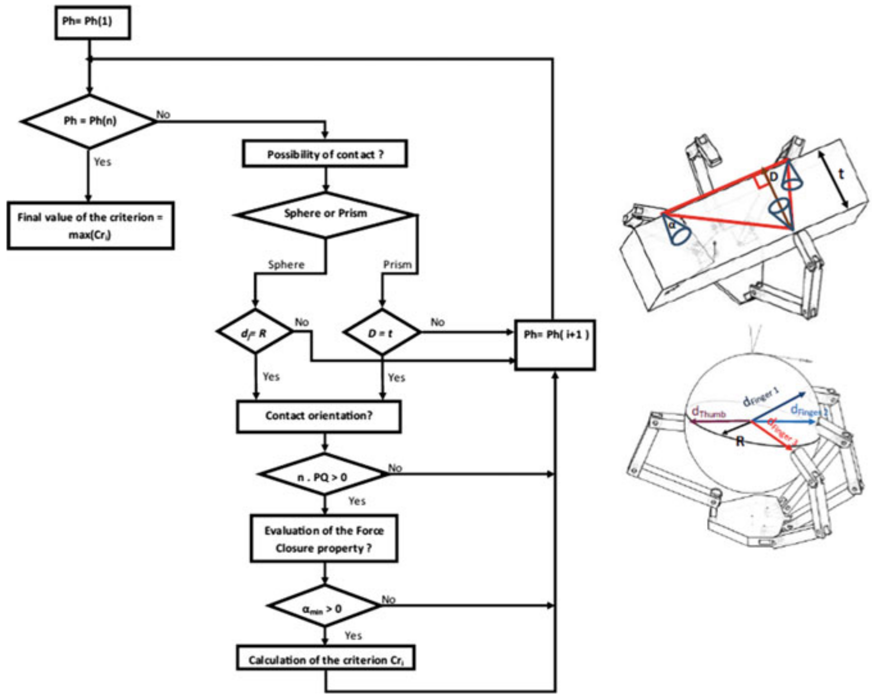


**Fig. 1.8** Computing flowchart of the criterion evaluating the grasp quality

The algorithm presented on Fig. 1.8 is implemented to handle two simple geometric shapes: the sphere and the prism. The sphere is located on the center of the palm. For the sphere, the distances $d_k$ are computed between the sphere center and the fingertips of the four fingers. The radius of the sphere is noted by $R$ as shown on Fig. 1.8. The contact is possible if and only if:

$$d_k = R \text{ for } k \in [\text{Finger 1},\ \text{Finger 2},\ \text{Finger 3},\ \text{Thumb}] \tag{1.5}$$

For the prism with a thickness $t$, as illustrated on Fig. 1.8, the grasp is considered done with three fingers. The three contact points between the fingertips, of the fingers 1 and 3 and the thumb, and the prism surfaces describe a triangle. The altitude of this triangle is noted by $D$. The contact is possible if and only if:

$$D = t \tag{1.6}$$

If the contact occurs, then it should be oriented toward the inside of the object, which means that the fingers are located outside the object. This constraint is verified through the computing of the scalar product between the normal to the surface contact,

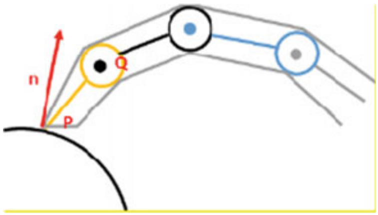


**Fig. 1.9** Contact between the fingertips and the object

**n**, and the last phalanx vector, **PQ** (see Fig. 1.9). The contact is correctly oriented, fingers outside the object, if and only if:

$$\mathbf{n} \cdot \mathbf{PQ} > 0 \tag{1.7}$$

For the evaluation of the force closure property, we use the Li Algorithm. The Li Algorithm computes an angle $\alpha$ that evaluates how far the configuration of the grasp is from the loss of the property. It is based on the evaluation of the friction cones disposition at the contact points [11]. Our criterion uses the angle $\alpha$ as described on Fig. 1.9. The grasp is "Force Closure" if the smallest angle of the friction cone is non-null.

$$\alpha_{min} > 0 \tag{1.8}$$

The criterion used to determine the best geometry is the evaluation criterion called "Volume of the ellipsoid in the wrench space" which defines the global contribution of all the contact forces [12]. This criterion is defined by the grasp matrix $G$, which depends on the position of the contact points between the fingertips and the objects surfaces, computed thanks to the coordinates given below. It is noted $Cr$.

The matrix G establishes the relation between the fingertip forces $f$ and the net wrench applied on the object $\omega$, and the relation between velocities at the contact points $v$ and the twist $\dot{x}$. We suppose that $v$ is equal to zero since the object is motionless.

$$\omega = G \cdot f \text{ and } v = G^T \cdot \dot{x} \tag{1.9}$$

$$Cr = \det\left(G \cdot G^t\right) \tag{1.10}$$

The architecture of the hand is presented on Fig. 1.10, with the different parameters appearing in the expressions of the criteria used in the evaluation process of the hand workspaces.

The coordinates of the fingertips of the four fingers are given by the following equations:

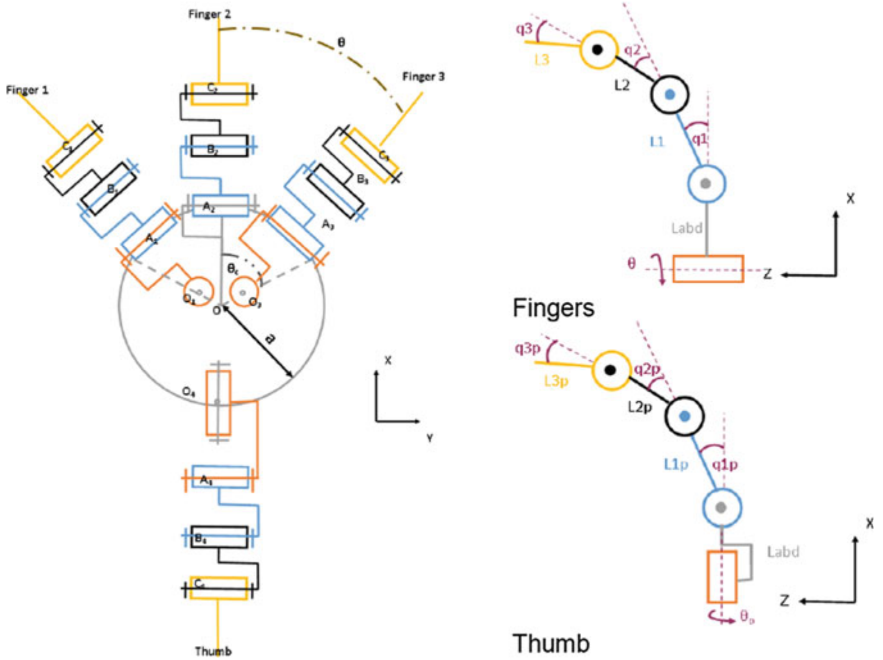


**Fig. 1.10** Architecture and parameters of the robotic hand

| | |
|---|---|
| $\begin{pmatrix} x_{Finger\,1} \\ y_{Finger\,1} \\ z_{Finger\,1} \end{pmatrix} = R(\theta, z) * \left[ \begin{pmatrix} L_{abd} \\ 0 \\ 0 \end{pmatrix} + M \right] + \begin{pmatrix} (a - L_{abd}) * \cos(\theta_c) \\ (a - L_{abd}) * \sin(\theta_c) \\ 0 \end{pmatrix}$ | $\begin{pmatrix} x_{Finger\,2} \\ y_{Finger\,2} \\ z_{Finger\,2} \end{pmatrix} = M + \begin{pmatrix} a \\ 0 \\ 0 \end{pmatrix}$ |
| $\begin{pmatrix} x_{Finger\,3} \\ y_{Finger\,3} \\ z_{Finger\,3} \end{pmatrix} = R(-\theta, z) * \left[ \begin{pmatrix} L_{abd} \\ 0 \\ 0 \end{pmatrix} + M \right] + \begin{pmatrix} (a - L_{abd}) * \cos(\theta_c) \\ -(a - L_{abd}) * \sin(\theta_c) \\ 0 \end{pmatrix}$ | $\begin{pmatrix} z_{thumb} \\ y_{thumb} \\ z_{thumb} \end{pmatrix} = N_i + \begin{pmatrix} -a \\ 0 \\ 0 \end{pmatrix} \; for\; i = 1, 2\; or\; 3$ |

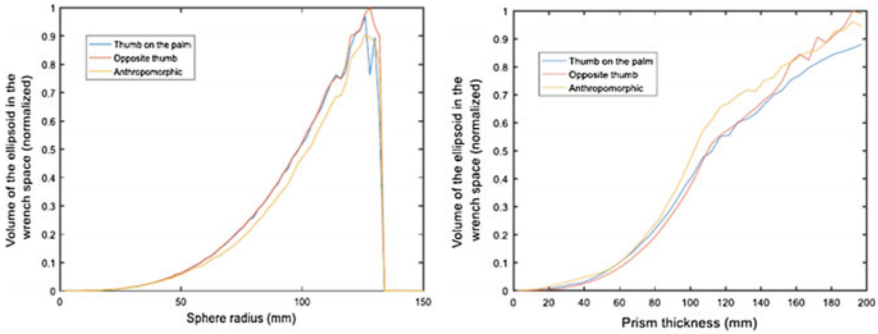


**Fig. 1.11** Evolution of the criterion for different sizes of grasped objects

Where $\theta_c$ is a constant and $q_{1i}, q_{2i}, q_{3i}, \theta_i, q_{1pi}, q_{2pi}, q_{3pi}, \theta_{pi}$ are the joints parameters whose values vary between the joint limits presented on Table 1.4.

The matrix $M$ is defined as follows:

$$M = \begin{pmatrix} L1 * \cos(q_1) + L2 * \cos(q_1 + q_2) + L3 * \cos(q_1 + q_2 + q_3) \\ 0 \\ L1 * \sin(q_1) + L2 * \sin(q_1 + q_2) + L3 * \sin(q_1 + q_2 + q_3) \end{pmatrix}$$

The matrix $N_i$ is defined as follows for the three different placements of the thumb depicted on Table 1.3.

$$N_1 = \begin{pmatrix} \cos(\theta_p) * (L_{abd} + L1p * \cos(q_{1p}) + L2p * \cos(q_{1p} + q_{2p}) + L3p * \cos(q_{1p} + q_{2p} + q_{3p})) \\ \sin(\theta_p) * (L_{abd} + L1p * \sin(q_{1p}) + L2p * \sin(q_{1p} + q_{2p}) + L3p * \sin(q_{1p} + q_{2p} + q_{3p})) \\ L1p * \sin(q_{1p}) + L2p * \sin(q_{1p} + q_{2p}) + L3p * \sin(q_{1p} + q_{2p})) \end{pmatrix}$$

$$N_2 = \begin{pmatrix} \frac{\sqrt{2}}{2} & -\frac{\sqrt{2}}{2} & 0 \\ \frac{\sqrt{2}}{2} & \frac{\sqrt{2}}{2} & 0 \\ 0 & 0 & 1 \end{pmatrix} * N_1;$$

$$N_3 = \begin{pmatrix} L1p * \cos(q_{1p}) + L2p * \cos(q_{1p} + q_{2p}) + L3p * \cos(q_{1p} + q_{2p} + q_{3p})) \\ -\sin(\theta_p) * (L_{abd} + L1p * \sin(q_{1p}) + L2p * \sin(q_{1p} + q_{2p}) + L3p * \sin(q_{1p} + q_{2p} + q_{2p})) \\ \cos(\theta_p) * (L_{abd} + \cos(L1p * \sin(q_{1p}) + L2p * \sin(q_{1p} + q_{2p}) + L3p * \sin(q_{1p} + q_{2p} + q_{3p})) \end{pmatrix}$$

Figure 1.11 presents the normalized value of the criterion "Volume of the ellipsoid in the wrench space" *Cr*.

$$Cr = \frac{Cr}{\max(Cr)} \tag{1.11}$$

The criterion *Cr* is computed for different sizes of grasped objects. When the value is equal to zero, then it means that it is impossible to get a stable grasp.

One can see that the anthropomorphic placement of the thumb leads to slightly better prismatic grasp and slightly less good sphere grasp. The two other geometries, the cases 2 and 3, lead to very similar results. According to the obtained results, the geometry with the thumb on the palm is chosen as the more suitable solution. This third hand geometry presents the largest workspace, and covers the largest area over the palm. The chosen geometry is given on the third column of Table 1.3 and detailed on Fig. 1.10.

## 1.4 Conclusion and Future Work

In this paper, we were looking for a hand geometry that would suit the underwater archaeology. For that purpose, we studied the expert gesture, using motion capture system in simulated archaeological site. A new task taxonomy peculiar to submarine archaeologist's activity has been established.

From the data analysis of the joints evolution, the fingertips workspace and the joints velocity, we selected the hand geometry that will be able to realize all the archeology tasks identified. The more suitable geometry has been chosen among the three candidates geometries that are evaluated.

Two different criteria have been defined and implemented in this purpose: the workspace of the fingertips and the ability to make a stable grasp.

In future work, the optimal dimensions of the fingers and the palm will be investigated through an optimization problem. The under actuation will be also studied.

## Annex: Taxonomy of the Submarine Archaeology Task

| Task / Grasp name | Type | Opposition Type | Thumb Position | Virtual Fingers | 1 or 2 hands | Picture |
|---|---|---|---|---|---|---|
| Sweeping | Underaction | NA | Adducted | 2 to 4 | 1 |  |
| Scraping | Underaction | NA | Abducted | 2 to 4 | 1 |   |
| Checking out | Precision | Pad | Abducted | 2 | 1 |  |
| Shoveling | Precision | Palm | Abducted | 3 to 5 | 1 | 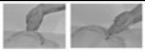 |
| Packaging light objects | Intermediate | Palm | Adducted | 3 to 4 | 1 |  |
| Packaging heavy objects | Power | Palm | Abducted | 6 to 10 | 2 |  |
| Cupped hand | Precision | Palm | Abducted | 3 to 5 | 1 |  |
| Locked cupped hand | Intermediate | Palm | Adducted | 3 to 5 | 1 |  |
| Large objects | Intermediate | Palm | Abducted | 6 to 10 | 2 |  |
| By the top | Precision | Pad | Adducted | 3 to 5 | 1 |  |
| Friable objects | Power | Palm | Adducted | 6 to 10 | 2 |  |

| Task / Grasp name | Type | Opposition Type | Thumb Position | Virtual Fingers | 1 or 2 hands | Picture |
|---|---|---|---|---|---|---|
| Two cupped hands | Intermediate | Palm | Abducted | 6 to 10 | 2 |  |
| Hand flat | Precision | Palm | Adducted | 3 to 5 | 1 |  |
| Extension type (F) | Power | Pad | Abducted | 2 to 5 | 1 |  |
| Palmar pinch (F) | Precision | Pald | Abducted | 2 | 1 |  |
| Tripod | Precision | Pad | Abducted | 3 | 1 |  |
| Medium wrap (F) | Power | Palm | Abducted | 3 to 5 | 1 |  |
| Writting tripod (F) | Precision | Side | Abducted | 2 to 3 | 1 | 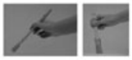 |
| Adducted thumb (F) | Power | Palm | Adducted | 2to 5 | 1 |  |
| Clamp | Power | Pad + phalanx | Abducted | 2 to 5 | 1 |  |
| Delicate clamp | Intermediate | Pad | Adducted | 2 to 3 | 1 |  |

(F) : grasp presented in Feix taxonomy

## References


1. Cutkosky, M.R.: On grasp choice, grasp models, and the design of hands for manufacturing tasks. IEEE Trans. Robot. Autom. **5**(3), 269–279 (1989)
2. Feix, T., Pawlik, R., Schmiedmayer, H.B., Romero, J., Kragic, D.: A comprehensive grasp taxonomy. In: Robotics, Science and Systems: Workshop on Understanding the Human Hand for Advancing Robotic Manipulation, pp. 2–3, June 2009
3. Bullock, I.M., Zheng, J.Z., De La Rosa, S., Guertler, C., Dollar, A.M.: Grasp frequency and usage in daily household and machine shop tasks. IEEE Trans. Haptics **6**(3), 296–308 (2013)
4. Lane, D.M., Davies, J.B.C., Casalino, G., Bartolini, G., Cannata, G., Veruggio, G., et al.: AMADEUS: advanced manipulation for deep underwater sampling. IEEE Robot. Autom. Mag. **4**(4), 34–45 (1997)
5. Meng, Q., Wang, H., Li, P., Wang, L., He, Z.: Dexterous underwater robot hand: HEU Hand II. In: Proceedings of the 2006 IEEE International Conference on Mechatronics and Automation, pp. 1477–1482. IEEE, June 2006
6. Khatib, O., Yeh, X., Brantner, G., Soe, B., Kim, B., Ganguly, S., Mullins, P.: Ocean one: a robotic avatar for oceanic discovery. IEEE Robot. Autom. Mag. **23**(4), 20–29 (2016)
7. Bemfica, J.R., Melchiorri, C., Moriello, L., Palli, G., Scarcia, U., Vassura, G.: Mechatronic design of a three-fingered gripper for underwater applications. IFAC Proc. Vol. **46**(5), 307–312 (2013)

8. Kapandji, A.: Clinical test of apposition and counter-apposition of the thumb. Annales de chirurgie de la main: organe officiel des societes de chirurgie de la main **5**(1), 67–73 (1985)
9. Mnyusiwalla, H., Vulliez, P., Gazeau, J.P., Zeghloul, S.: A new dexterous hand based on bio-inspired finger design for inside-hand manipulation. IEEE Trans. Syst. Man Cybern. Syst. **46**(6), 809–817 (2016)
10. Mnyusiwalla, H.: Qualité de prise dans le contexte de la planification de mouvements de préhension et de manipulation dextre en robotique. Doctoral dissertation, Poitiers (2016)
11. Jin, J.-W., Liu, M.-H., Li, H.: A new algorithm for three-finger force-closure grasp of polygonal objects. In: International Conference on Robotics and Automation, vol. 2, pp. 1800–1804 (2003)
12. Suárez, R., Cornella, J., Garzón, M.R.: Grasp quality measures. Institut d'Organització i Control de Sistemes Industrials (2006)

# Chapter 2
# A Vision-Based Strategy for a Cost-Effective Flexible Robotic Assembly System Without Using RCC Devices and Compliant Control

**C. Y. Weng and I. M. Chen**

**Abstract** This paper aims to provide a vision-based self-adaptive strategy to cope with the uncertainties in a cost-effective robotic assembly system without the adoption of RCC devices and compliant control. Several assumptions are given in the first stage for the adaption in practical manufacturing. Then various approaches are taken in our proposed robotic assembly system for dealing with a classical peg-in-hole insertion process. In the end, the realistic implementations are carried out to verify the effectiveness of our strategy.

**Keywords** Computer vision · Robotic assembly · Intelligent system

## 2.1 Introduction

Based on the fulfillment of sustainability, the demands of industrial robot technology from high-growth industries are increasing [1]. As a result, the potential of the utilization of industrial robots to realize the feature of flexibility in automation manufacturing has become a main stream view, the value of investing efforts in the robotic system integration is a forward-looking consideration. In practical, the main advantage of the deployment of industrial robots is that they can be applied to a wide range of feasible industrial applications have them be properly programmed and integrated into manufacturing systems. Most industrial robots can be equipped with various peripherals, such as different sensors or computer vision systems, providing the robots some utilizable feedback information on their decision processes, thereby improving the robots' abilities to cope with quite a few more arduous tasks which may need a higher precision guidance or an object recognition process [2]. In most circumstances, the elements in a robotic integration system are an overhead which cannot be ignored. The better the peripherals employed, the better the performances of the robotic systems are presented. Sometimes, however, we can adopt

C. Y. Weng · I. M. Chen (✉)
School of Mechanical and Aerospace Engineering, Nanyang Technological University, Singapore, Singapore
e-mail: michen@ntu.edu.sg



R. Yang et al. (eds.), *Robotics and Mechatronics*, Mechanisms and Machine Science 72, https://doi.org/10.1007/978-3-030-17677-8_2

with a simpler and cost-effective measure and peripheral equipment to implement a robotic task, which can save considerable time and cost for us. In view of this, this paper proposes a vision-based strategy for a cost-effective flexible robotic assembly system without using RCC devices (hard 1 DOF grippers produced by 3D printing) and compliant control (no path searching behavior during assembling).

## 2.2 Assumptions

The implemented strategy is based on several assumptions made to satisfy the realistic flexible manufacturing scenarios. The assumptions are given as follows:

1. In most assembly manufacturing workstations, the assembly parts are first transported to the workstations after they are produced. Plus, after the completion of assemblies, those assemblies are transported to other workstations. This kind of behavior is commonly realized through conveyors. Therefore, we can assume that there is a virtual transportation system in our robotic workspace, that is, the assembly parts can appear at the beginning and disappear in the end.
2. The assembly parts are always presented in workstations with pre-determined positions and orientations by the orienting systems to not only manifest the effectiveness of the picking processes of robots but also facilitate the programming of engineers. Furthermore, different forms of the presentation of assembly parts are considered in realistic manufacturing scenarios, such as the utilization of feeders, pallets, and magazines. In view of this, we simply conclude the features of the presenting methods mentioned previously and assume that there is a week presenting system to assist the robot, that is, the assembly parts appear in a random position in each area, so do their orientation (only the orientation along the normal direction of the workspace plane are random).
3. Intuitively, from the manual assembly of the scene to consider, workers generally know what the product is to be assembled as well as the motion sequences to assemble the product. As a result, we can assume the assembly parts and their assembly processes are given to the robotic system as prior knowledge.

## 2.3 Methodologies and Results

Based on the assumptions made previously, we design the vision-based strategies inspired by the action of charging a cell phone. An ordered motion sequence of getting a wire terminal and connecting it on a cell phone is given as follows:

1. Find the rough position of the cell phone.
2. Determine how to pick up the cell phone.
3. Pick up the cell phone.
4. Find the rough position of the charging terminal.

5. Determine how to pick up the charging terminal.
6. Pick up the charging terminal.
7. Place (or fix) the cell phone.
8. Insert the charging terminal into the cell phone connector.
9. If we find that the charging terminal cannot be plugged into the cell phone connector, we will generally re-confirm the pose of the charging terminal by eyes, and then re-insert it again.

In summary of the above steps, we can conclude that the main vision-based strategies are global detection, local detection, and error detection. However, we change the step of error detection to an offline strategy to reduce the waste of time caused by pose error in our robotic task, that is, we move the step to the beginning of the insertion step. The detailed approaches are provided in the following sections.

### 2.3.1 Global Detection

The goal of global detection is to search the whole workspace plane and find the rough position of every assembly part presented. In this step, if any of the assembly parts is missing, the next step will not proceed by the robotic system. This approach is realized by PCL with the utilization of point cloud data [3]. The working principle is as follows:

1. Transform the point cloud data $p \in \mathbb{R}^{3\times n}$ to the robot base coordinate $q \in \mathbb{R}^{3\times n}$, which is also the global coordinate:

$$q = \begin{bmatrix} q_x \\ q_y \\ q_z \end{bmatrix} = T_{base}^{sensor} p, \tag{2.1}$$

   where $n$ is the number of the points in point cloud data; $T_{base}^{sensor}$ is the homogeneous transformation matrix from the robot base coordinate to the sensor coordinate.

2. Get the point cloud data only on the workspace plane by using the cartesian threshold filter:

$$\begin{aligned} q_i' &= \begin{bmatrix} q_{xi}' & q_{yi}' & q_{zi}' \end{bmatrix}^{\mathrm{T}} \\ q_{xi}' &= \begin{cases} q_{xi}, & q_{xi} \in [X_L, X_U] \\ NAN, & otherwise \end{cases} \\ q_{yi}' &= \begin{cases} q_{yi}, & q_{yi} \in [Y_L, Y_U] \\ NAN, & otherwise \end{cases} \\ q_{zi}' &= \begin{cases} q_{zi}, & q_{zi} \in [Z_L, Z_U] \\ NAN, & otherwise \end{cases} \end{aligned}, \tag{2.2}$$